

**To cite this article:** LI S J, XU C Q, LIU J L, et al. Tracking control of ships based on ADRC—MFAC [J/OL]. Chinese Journal of Ship Research, 2024, 19(1). <http://www.ship-research.com/en/article/doi/10.19693/j.issn.1673-3185.03226> (in both Chinese and English).

**DOI:** 10.19693/j.issn.1673-3185.03226

# Tracking control of ships based on ADRC—MFAC



LI Shijie<sup>1,2,5</sup>, XU Chengqi<sup>5</sup>, LIU Jialun<sup>\*1,2,3,4</sup>, XU Ziqian<sup>5</sup>, MENG Fanbin<sup>2,6</sup>

1 State Key Laboratory of Maritime Technology and Safety,  
Wuhan University of Technology, Wuhan 430063, China

2 Laboratory of Science and Technology on Marine Navigation and Control,  
China State Shipbuilding Corporation, Tianjin 300131, China

3 Intelligent Transportation Systems Research Center, Wuhan University of Technology, Wuhan 430063, China

4 National Engineering Research Center for Water Transport Safety, Wuhan 430063, China

5 School of Transportation and Logistics Engineering, Wuhan University of Technology, Wuhan 430063, China

6 Tianjin Navigation Instruments Research Institute, Tianjin 300131, China

**Abstract:** [Objective] This paper aims to investigate the complex influence of environmental disturbances on unmanned surface vehicles (USVs) under real ocean conditions, and control USVs to overcome disturbances and realize path following. [Methods] An improved active disturbance rejection controller (ADRC) based on the model-free adaptive control (MFAC) law (ADRC-MFAC) is proposed to establish the non-linear relationship between the input data (rudder angle) and output data (heading angle, angular velocity), and identify the unknown disturbances of the system. In this way, stable heading control can be achieved. Combined with the adaptive line-of-sight (LOS) guidance law, it achieves accurate tracking control through dynamic heading control. [Results] The simulation results show that the controller can control USVs to approach the preset path quickly and achieve a desirable tracking control effect under complex disturbances. [Conclusion] The research results do not depend on the specific model of USV and can provide valuable references for ship tracking control.

**Key words:** tracking control; ADRC algorithm; MFAC algorithm; data-driven control

**CLC number:** U664.82

## 0 Introduction

In recent years, rapid development of modern technologies like communication and computer has greatly promoted research and application of intelligent ships. One of the key steps to develop an intelligent ship is to perceive information on the ship itself and its surrounding environment to issue commands to control its action of each time according to its task, so as to realize autonomous motion control<sup>[1]</sup>. Different from other controlled systems, ships are characterized by the non-linearity, large inertia, and long-time delay of motion. As a result, they are easily disturbed by external factors such as winds, waves, and currents during navigation. Moreover, ships may deviate from their expected states and preset tracks or even lose control under

complex environmental disturbances<sup>[2]</sup>. Thus, how to overcome influence of disturbances is an important problem to be solved in motion control of ships.

At present, many effective control algorithms are available for motion control of intelligent ships under complex disturbances. For example, in view of ship course keeping, considering influence of winds and waves on ship heading, according to dynamic properties of steering gears and fully-nonlinear static maneuvering characteristics of ships, Witkowska et al.<sup>[3]</sup> proposed an algorithm of adaptive backstepping control to improve system performance by dynamic adjustment of nonlinear systems. In view of path following and control of ships, Sun et al.<sup>[4]</sup> designed a sliding-mode control

algorithm based on parameter estimation. Considering unknown environmental disturbances, this algorithm enhanced system robustness and adaptively controls ship motion. In view of rolling stability of ships, Jimoh et al. [5] proposed a control strategy for model prediction based on disturbance observers, which reduced influence of modeling errors and complex disturbances on systems by predicting system uncertainty.

Most of the existing algorithms are model-based control algorithms. In such algorithms, it is necessary to establish dynamic models equivalent to actual motion of ships based on accurate analysis of stress characteristics and dynamic behavior of the ships, and then design specific controllers according to requirements of control tasks. In practical applications, it is difficult to fully satisfy system assumptions during modeling. As a result, model accuracy can hardly be guaranteed, which greatly limits performance of model-based control algorithms<sup>[6]</sup>. By comparison, using data-driven algorithms to design controllers based on online/offline input/output data of systems can effectively deal with inaccurate modeling of nonlinear systems<sup>[7]</sup>.

Based on data driving, regarding all uncertainties acting on a controlled system as unknown disturbances, active disturbance rejection control (ADRC) estimates and compensates for such unknown disturbances in real time according to input/output information of the system [8]. Due to its simple structure and easy implementation in engineering, ADRC has been applied in many fields, such as robots [9] and wind farms [10]. In terms of ship control, ADRC has also been studied extensively. Applying ADRC to dynamic positioning control of ships, Xiong and Jin et al. [11] verified that the algorithm performed well in dynamic control of ships under strong disturbances, which was able to improve disturbance rejection of systems. With ADRC, based on adaptive line-of-sight (LOS) guidance, Huang [12] optimally controlled path following of ships. According to relevant research, although ADRC can well deal with disturbances to ship navigation in complex environment, it still has some problems, such as frequent steering and excessively large rudder amplitude.

To meet actual steering requirements and reduce steering frequency and amplitude, Liao et al. [13] controlled ship's heading through model-free adaptive control (MFAC). With redefinition of system

outputs, by introducing angular velocity to restrict variations of rudder angles, they improved steering stability and adaptability. MFAC is data-based, and its principle is to establish an equivalent dynamic linearized data model at each dynamic operating point in a closed-loop system and then design a controller based on the virtual data model [14]. Therefore, it is highly robust and has widely been used in wide-area power systems [15] and for handling network-induced delay and packet dropout [16].

In view of ship motion control, for achieving accurate heading and tracking control, by introducing MFAC to improve ADRC, this paper proposed an ADRC–MFAC-based control algorithm. At first, LOS guidance was used to follow the desired track, and nonlinear relationship between ship's inputs (rudder angles) and outputs (heading angles and angular velocity) was dynamically identified by MFAC. On this basis, with the ship's heading angle and angular velocity as comprehensive outputs, angular velocity was controlled to remain at small values all the time while minimizing output heading deviations, to ensure smooth navigation of the ship. Then, with the comprehensive goal of controlling the ship to overcome complex environmental disturbances and navigate stably in an expected state, an ADRC algorithm was designed. Moreover, based on the observation of the navigation state of the ship, internal and external disturbances to the ship were estimated in real time and compensated for accordingly. Finally, simulation was carried out according to the designed controller to verify effectiveness of the algorithm.

## 1 Mathematical model of ship motion

### 1.1 Coordinate system for ship motion

Due to its high complexity, ship motion is represented by a ship motion coordinate system. As shown in Fig. 1,  $o-xyz$  is a body-fixed coordinate system of the ship, with  $ox$  pointing to the bow,  $oy$  pointing to the starboard, and  $oz$  pointing to the bottom. The ship moves linearly and rotates along  $ox$ ,  $oy$ , and  $oz$  directions, respectively. Thus, six independent coordinates (i. e. the six-degree-of-freedom coordinates: surging  $u$ , swaying  $v$ , heaving  $w$ , rolling  $p$ , pitching  $q$ , and yawing  $r$ ) are needed to determine motion attitudes of the ship. In the ship heading and tracking control, only the ship's

heading angle  $\varphi$  and actual coordinates  $(x, y)$  are the key control parameters. Thus, ignoring influence of heaving, rolling, and pitching, this paper only considered surging, swaying, and yawing. As a result, ship motion was reduced to a mathematical model only considering the three degrees of freedom of  $u$ ,  $v$ , and  $r$ . On this basis, a controller was designed.

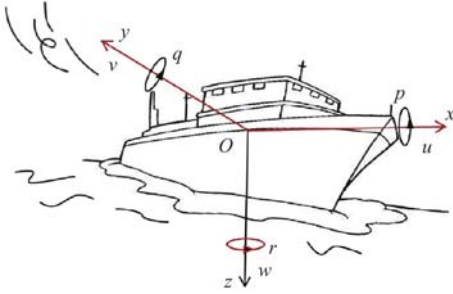


Fig. 1 Body-fixed frame of ship

### 1.2 Mathematical model of ship motion

In this paper, the mathematical model of ship motion is based on the three degrees of freedom,  $u$ ,  $v$ , and  $r$ . Ship motion is expressed by longitudinal velocity, transverse velocity, and yawing angular velocity. The under-actuated three-degree-of-freedom ship motion model [17] used in this paper is given by:

$$\begin{cases} \dot{x} = u \cos \varphi - v \sin \varphi + u_c \cos \varphi_c \\ \dot{y} = u \sin \varphi + v \cos \varphi + u_c \sin \varphi_c \\ \dot{\varphi} = r \\ \dot{u} = [X_H + X_P + X_R + X_E + (m + m_x)vr] / (m + m_x) \\ \dot{v} = [Y_H + Y_P + Y_R + Y_E - (m + m_y)ur] / (m + m_y) \\ \dot{r} = (N_H + N_P + N_R + N_E) / (J_{xx} + J_{zz}) \end{cases} \quad (1)$$

where  $[x, y, \varphi]^T$  is a position vector, in which  $x, y$ , and  $\varphi$  denote displacement and heading angle in the surging and swaying directions, respectively;  $[u, v, r]^T$  is a velocity vector, in which  $u, v$ , and  $r$  represent longitudinal velocity, transverse velocity, and yawing angular velocity, respectively;  $u_c$  and  $\varphi_c$  denote the velocity and direction angle of current flow, respectively;  $X, Y$  and  $N$  represent the force and moment along a coordinate axis; the subscripts H, P, R, and E represent external disturbances from the hull, the propeller, the rudder, and the wind-wave-current;  $m$  is mass of the ship;  $m_x$  and  $m_y$  are the components of additional mass of water in  $x$  and  $y$  directions in the body-fixed coordinate system;  $J_{xx}$  is additional moment of inertia regarding the  $x$  axis in the body-fixed coordinate system;  $J_{zz}$  is additional moment of inertia regarding the  $z$  axis in the body-fixed coordinate system.

### 1.3 Analysis of LOS guidance

In this paper, a LOS guidance algorithm was used to guide the ship to follow the preset track. This algorithm is independent of the mathematical model of a controlled system, featuring easy parameter adjustment, low calculation loads, high stability, and easy implementation. Thus, it is widely used in studying tracking control of ships [18].

Fig. 2 illustrates the basic principle of LOS guidance. Usually, the ideal track of a ship is determined by a series of waypoints. During motion control, an expected heading angle is calculated according to the deviation between the current position of the ship and its ideal track. Moreover, the actual heading angle is controlled by the control algorithm to converge to the expected heading angle, so as to eliminate the heading deviation. In the figure,  $P_n(x_n, y_n)$  and  $P_{n+1}(x_{n+1}, y_{n+1})$  are the preset  $n$ -th and  $(n+1)$ -th waypoints, respectively;  $O$  is the position of the mass point of the ship;  $P_{los}$  is the target point at this moment.  $P_{los}$  is the position where the dynamic circle with the ship as the center and the variable parameter  $R_0$  as the radius intersects the ideal track and is closer to the next waypoint. Its coordinates can be solved by:

$$\begin{cases} (x_{los} - x)^2 + (y_{los} - y)^2 = R_0^2 \\ (x_{los} - x_n) / (y_{los} - y_n) = (x_{n+1} - x_{los}) / (y_{n+1} - y_{los}) \end{cases} \quad (2)$$

In this case, the vector  $OP_{los}$  pointing from the ship itself to the target point is called a LOS vector. The direction angle of the LOS vector is called a LOS angle  $\varphi_{los}$ . The difference between the ship heading angle  $\varphi$  and the LOS angle  $\varphi_{los}$  is called a heading deviation angle  $\theta$ . The LOS angle, that is, the expected heading angle  $\varphi_{los}(k)$  at time  $k$ , can be calculated according to the deviation between the ship's current position  $(x, y)$  and the target position  $(x_{los}, y_{los})$ , as shown in Eq. (3).

$$\varphi_{los}(k) = \arctan((y_{los} - y) / (x_{los} - x)) \quad (3)$$

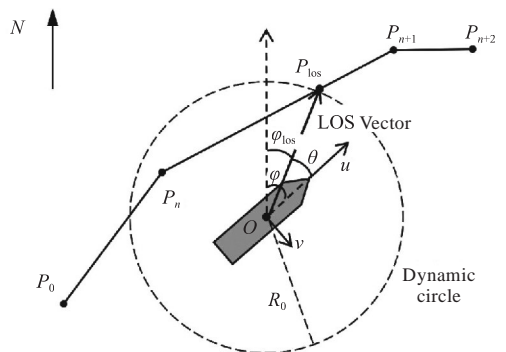


Fig. 2 Principle of LOS guidance law

The expected heading angle at each time during the control is calculated according to the principle of LOS guidance, and then complex tracking control is realized by dynamic heading control.

## 2 ADRC-MFAC controller design

Due to complex environmental disturbances to ship navigation, it is difficult to achieve stable navigation control in the absence of an accurate mathematical model. According to LOS guidance, this paper transformed tracking control into heading control. By introducing MFAC that redefines outputs, it established nonlinear relationship of a ship's heading angle and angular velocity to its rudder angle, and then controlled the ship's heading by controlling the rudder angle. In addition, an MFAC-based ADRC algorithm was designed to compensate for complex disturbances to the ship to autonomously counteract the influence of disturbances on ship motion, so as to control ship motion accurately. Fig. 3 illustrates the overall structure of the tracking control system.

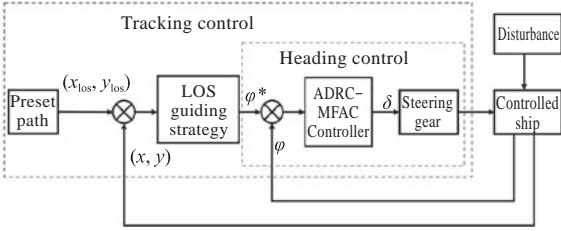


Fig. 3 Block diagram of tracking control system

Fig. 4 illustrates the structure of the ADRC-MFAC-based ship tracking controller. A traditional ADRC consists of four parts: tracking differentiator (TD), nonlinear state error feedback (NLSEF), extended state observer (ESO) and disturbance compensator. With MFAC introduced in this paper, when ADRC works, the expected heading angle  $\varphi^*(k)$  tracked by TD and the state observation vector  $[\alpha_1, \alpha_2, f]^T$  from ESO regarding the actual heading angle  $\varphi(k)$  are input into the MFAC control law (where  $f$  represents the total disturbance, and  $\alpha_1$  and  $\alpha_2$  are system state variables). According to the deviation  $\Delta y$  between the current and the expected states of the ship, the initial controlled rudder angle  $u_{MFAC}$  is given. Then, the final controlled rudder angle  $\delta$  after disturbance compensation is obtained through the disturbance compensation factor  $b_0$ . This ensures that the control system can obtain more reasonable rudder angles and reduce rudder-

angle variation frequency while compensating for disturbances autonomously.

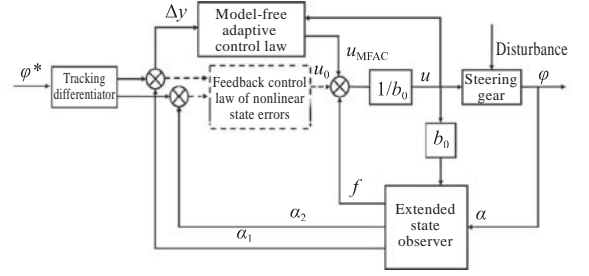


Fig. 4 Block diagram of ADRC-MFAC controller

### 2.1 Tracking differentiator (TD)

The ADRC-MFAC controller aims to control the ship heading angle  $\varphi(k)$  to converge to the expected one  $\varphi_{10s}(k)$ . TD can quickly track the input signal  $\varphi_{10s}(k)$  to reduce impact on the system at the initial stage, thus effectively solving the contradiction between overshoot and rapidity. Let the input and output signals of TD be  $c(k)$  and  $c_i(k)$  ( $i = 1, 2$ ), respectively. Then, relationship between the two is given by:

$$\begin{cases} c_1(k+1) = c_1(k) + hc_2(k) \\ c_2(k+1) = c_2(k) + hv \end{cases} \quad (4)$$

Where  $c_1(k)$  is the tracking signal of the input signal  $c(k)$ ;  $c_2(k)$  is the first-order differential of  $c_1(k)$ ;  $h$  is an integration step;  $v = \text{fhan}(c_1 - c, c_2, l, h_0)$  is the multifactorial function of time-optimal control defined by the ADRC algorithm [8]. It is used to process input signals to avoid fluttering. The calculation formula is given by

$$\begin{cases} d = lh_0, d_0 = h_0d \\ s = c_1 - c + h_0c_2, a_0 = \sqrt{d^2 + 8l|s|} \\ a = \begin{cases} c_2 + (a_0 - d)/2, & |s| > d_0 \\ c_2 + s/h_0, & |s| \leq d_0 \end{cases} \\ \text{fhan} = - \begin{cases} l\text{sign}a, & |a| > d \\ la/d, & |a| \leq d \end{cases} \end{cases} \quad (5)$$

where  $l$  is a velocity factor, which determines the tracking velocity. A greater  $l$  leads to a higher velocity of  $c_1(k)$  in tracking the input signal  $c(k)$ ;  $s$  is an error factor, which reflects the state of TD in tracking the actual input signal;  $h_0$  is a new variable independent of the integration step  $h$ . An appropriate parameter  $h_0$  selected, which is greater than  $h$ , can eliminate overshoot in the process of the heading angle approaching the expected value. And  $d, d_0, a$  and  $a_0$  are all intermediate variables determined by the velocity factor  $l$ , the step variable  $h_0$  and the error factor  $s$ .

### 2.2 Extended state observer (ESO)

The ADRC–MFAC controller needs to accurately identify the actual heading angle  $\varphi(k)$  of the ship to estimate and compensate for the heading-angle offset  $e$  caused by internal and external disturbances of the system. Using ESO can ensure certain accuracy of the estimated  $\varphi(k)$  and the total internal and external disturbances of the system. Define the state input  $\varphi(k)$  of the system as  $\alpha$ . Let  $\alpha_1 = \alpha$ ,  $\alpha_2 = \alpha_1^{(1)}$ , and  $\alpha_3 = \alpha_2^{(1)} = f$ . Specifically,  $\alpha_1$  and  $\alpha_2$  are state variables of the system;  $\alpha_3 = f$  is an extended state variable of the system. Generally, ESO can be expressed as

$$\begin{cases} e = \hat{\alpha}_1 - \alpha \\ \dot{\hat{\alpha}}_1 = \hat{\alpha}_2 - \beta_{01}e \\ \dot{\hat{\alpha}}_2 = \hat{f} - \beta_{02}e + b_0u(k-1) \\ \dot{\hat{f}} = -\beta_{03}e \end{cases} \quad (6)$$

where  $\hat{\alpha}_i (i = 1, 2)$  and  $\hat{f}$  are the estimated values of the system state  $\alpha_i (i = 1, 2)$  and the total internal and external disturbance  $\alpha_3 = f$  of the system;  $\dot{\hat{\alpha}}_i (i = 1, 2)$  is the first-order differential of  $\hat{\alpha}_i (i = 1, 2)$ ;  $\dot{\hat{f}}$  is the first-order differential of  $\hat{f}$ ;  $u(k-1)$  is the final output rudder angle after disturbance compensation at the pervious moment;  $\beta_{01}$ ,  $\beta_{02}$  and  $\beta_{03}$  are gain parameters of output-error correction. Appropriate selection of adjustable gain parameters can make each state variable  $\hat{\alpha}_i$  well track the state variable  $\theta_i$  of the system. In this paper, a bandwidth coefficient  $w_0$  was set to adjust the gain parameters:  $\beta_{01} = 3w_0$ ,  $\beta_{02} = 3w_0^2$ , and  $\beta_{03} = w_0^3$ .

### 2.3 Model-free adaptive controller (MFAC)

Fig. 5 illustrates the structure and principle of MFAC. In the figure,  $y(k)$  represents an output state of the controlled system (depending on the specific controlled target);  $y^*(k+1)$  is the expected output at time  $k+1$ ;  $u(k)$  is an output control command;  $Z^{-1}$  represents reciprocal calculation.

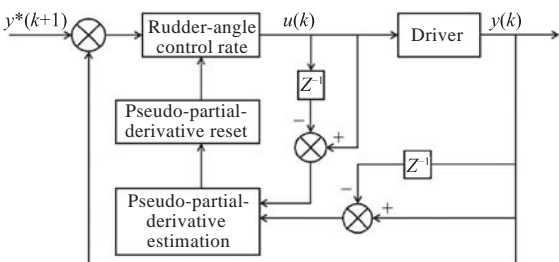


Fig. 5 Structure diagram of MFAC controller

In a conventional MFAC algorithm, the rudder-angle command  $u(k)$  of the ship at any time  $k$  is

defined as the system input and the actual heading angle  $\varphi(k)$  as the system output. On this basis, the nonlinear relation function  $f(\cdot)$  between the system input and output is generally constructed with the following discrete form:

$$\begin{aligned} \varphi(k+1) = f[\varphi(k), \varphi(k-1), \dots, \varphi(k-k_\varphi), \\ u(k), u(k-1), \dots, u(k-k_u)] \end{aligned} \quad (7)$$

where  $k_\varphi$  and  $k_u$  are unknown parameters.

During the control, overhigh angular velocity and over-quick heading variation of a ship can easily result in overshoot, making it difficult to keep heading angles stably in a desired state. Therefore, considering the influence of angular velocity on the system, this paper redefines the system output as  $y(k) = \varphi(k) + Kr(k)$ , where  $\varphi(k)$  is the actual heading angle of the ship;  $r(k)$  is angular velocity of the ship;  $K$  is the weight coefficient of angular velocity. As the original system input  $\varphi(k)$  is replaced by the new system input  $y(k)$ , relationship between the input and output of the new system is given as follows:

$$\begin{aligned} y(k+1) = f[y(k), y(k-1), \dots, y(k-k_y), \\ u(k), u(k-1), \dots, u(k-k_u)] \end{aligned} \quad (8)$$

where  $f(\cdot)$  is the unknown nonlinear relation function defined in this paper;  $k_y$  is an unknown parameter. In view of the unknown nonlinear relationship between the input and output of the system, this paper put forwards the following hypotheses.

Hypothesis 1: The input and output of Eq. (8) are observable and controllable. In other words, for the expected output signal  $y^*(k+1)$  at time  $k+1$ , there is a bounded and feasible input signal  $u^*(k)$  for rudder-angle control at time  $k$ . After the system executes the control command, its actual output is equal to the expected one.

Hypothesis 2: The nonlinear relation function  $f(\cdot)$  has a partial derivative with respect to the input control signal  $u(k)$  of the system and the partial derivative is continuous.

Hypothesis 3: The system satisfies the generalized Lipschitz continuity. In other words, for  $\Delta u(k) \neq 0$  at any time  $k$ , we have

$$|\Delta y(k+1)| \leq b|\Delta u(k)| \quad (9)$$

where  $\Delta y(k+1) = y(k+1) - y(k)$ ;  $\Delta u(k) = u(k) - u(k-1)$ ;  $b$  is a constant greater than 0.

**Theorem 1:** If the system satisfies the above hypotheses 1–3, then in the case of  $\Delta u(k) \neq 0$ , there will be a specific quantity  $\gamma(k)$  satisfying the following condition:

$$|\Delta y(k+1)| \leq \gamma(k)|\Delta u(k)| \quad (10)$$

where  $|\gamma(k)| \leq b$ . The unknown quantity  $\gamma(k)$  is defined as a pseudo partial derivative.

The dynamic linearized model of system output can be obtained from Theorem 1 as follows:

$$y(k+1) = y(k) + \gamma(k)\Delta u(k) \quad (11)$$

The criterion function of control input is defined as

$$J(u(k)) = |y^*(k+1) - y(k+1)|^2 + \lambda |u(k) - u(k-1)|^2 \quad (12)$$

where  $\lambda > 0$  is a weight coefficient of output;  $y^*(k+1) = \varphi_{\text{los}}(k+1) + Kr_d(k+1)$ ; the term  $|y^*(k+1) - y(k+1)|^2$  constrains the system output from converging to the desired state (specifically, the heading angle  $\varphi(k)$  converges to the expected  $\varphi_{\text{los}}(k)$ ; the angular velocity  $r(k)$  converges to the expected  $r_d(k)$ , and  $r_d(k) = 0$ ); the term  $\lambda |u(k) - u(k-1)|^2$  ensures that rudder angles are controlled smoothly without abrupt changes.

By substituting  $y(k+1)$  into the criterion function, calculating the derivative with respect to  $u(k)$ , and letting the result be 0, we can obtain the following control law of rudder angles:

$$u(k) = u(k-1) + [y^*(k+1) - y(k)] * \rho \gamma(k) / (\lambda + |\gamma(k)|^2) \quad (13)$$

where  $\rho$  is a step sequence.

The pseudo partial derivative  $\gamma(k)$  of the system is an unknown time-varying parameter, which cannot be directly applied to the input criterion function. Therefore, it can be estimated according to the input and output of the system. The estimation criterion function is given by

$$J(\gamma(k)) = |y(k) - y(k-1) - \gamma(k)\Delta u(k-1)|^2 + \mu |\gamma(k) - \hat{\gamma}(k-1)|^2 \quad (14)$$

where  $\mu > 0$  is a weight factor of the pseudo partial derivative;  $\Delta u(k-1) = u(k-1) - u(k-2)$ .

By calculating the extremum of the estimation criterion function with respect to the pseudo partial derivative  $\gamma(k)$ , we can obtain the estimation algorithm as follows:

$$\hat{\gamma}(k) = \hat{\gamma}(k-1) + [\Delta y(k) - \hat{\gamma}(k-1)\Delta u(k-1)] * \eta \Delta u(k-1) / (\mu + \Delta u(k-1)^2) \quad (15)$$

where  $\eta$  represents a step factor.

To ensure system stability, we define a reset algorithm for the estimated pseudo partial derivative  $\hat{\gamma}(k)$  as follows:

$$\hat{\gamma}(k) = \hat{\gamma}(1), \text{ if } |\hat{\gamma}(k)| \leq \varepsilon \text{ or } |\Delta u(k-1)| \leq \varepsilon \quad (16)$$

where  $\varepsilon$  is a sufficiently small positive number.

Finally, the estimated pseudo partial derivative  $\hat{\gamma}(k)$  is substituted into the rudder-angle control law to obtain a rudder-angle control command as follows:

$$u_{\text{MFAC}}(k) = u(k-1) + [y^*(k+1) - y(k)] * \rho \hat{\gamma}(k) / (\lambda + |\hat{\gamma}(k)|^2) \quad (17)$$

## 2.4 Disturbance compensation

According to the observed system state, the system calculates the initial rudder-angle control command  $u_{\text{MFAC}}(k)$  through the MFAC control law shown in Eq. (17). Finally, by compensation for the total disturbance  $f$  of the ESO system, the final rudder-angle control command is formed as follows:

$$u(k) = (u_{\text{MFAC}}(k) - f) / b_0 \quad (18)$$

## 3 Simulation analysis

### 3.1 Simulation Settings

To verify effectiveness of the designed ADRC–MFAC algorithm for ship tracking control, this paper set up a simulation environment on Matlab 2019a to study the self-developed KVLCC under-actuated tanker model ship. Fig. 6 illustrates the model ship. For the modeling of ship maneuvering, please refer to Reference [19]. Table 1 lists some parameters.

In the simulation, the ship was given an initial position of (0, 0), an initial heading angle of  $\varphi = 0^\circ$ , and an initial rudder angle of  $\delta = 0^\circ$ . Moreover, its longitudinal velocity was maintained at 1 m/s to avoid influence of velocity variation on heading. In view of the ADRC–MFAC algorithm proposed in this paper, conventional PID, MFAC, and ADRC algorithms were introduced to comparatively analyze the simulated heading and tracking control. Specifically, control parameters of traditional PID included the proportional coefficient  $k_p = 2.3$ , the integral coefficient  $k_i = 0.01$ , and the differential coefficient  $k_d = 9$ ; control parameters of MFAC included  $\lambda = 0.26$ ,  $\mu = 0.5$ ,  $\eta = 0.36$ ,  $\rho = 1.7$ , and  $K = 13$ ; control parameters of ADRC included  $l = 50$ ,  $h_0 = 2.5$ ,  $b_0 = 0.2$ ,  $w_0 = 0.45$ ; control parameters of ADRC–MFAC included  $l = 30$ ,  $h_0 = 1.5$ ,  $b_0 = 0.13$ ,  $w_0 = 0.5$ ,  $\lambda = 0.3$ ,  $\mu = 0.5$ ,  $\eta = 0.5$ ,  $\rho = 5$ , and  $K = 13$ .



Fig. 6 KVLCC2 under-actuated model ship

**Table 1 Particulars of KVLCC2 model ship**

| Parameter                       | Value   |
|---------------------------------|---------|
| Model scale                     | 1/45.7  |
| Ship length/m                   | 7.00    |
| Moulded breadth/m               | 1.16    |
| Moulded depth/m                 | 0.46    |
| Displacement/m <sup>3</sup>     | 3.27    |
| Ordinate of center of gravity/m | 0.25    |
| Fill factor                     | 0.810   |
| Propeller diameter/m            | 0.216   |
| Rudder span/m                   | 0.345   |
| Rudder area/m <sup>2</sup>      | 0.053 9 |

Table 2 lists the simulation tests and conditions. Specifically, a constant disturbance of  $N_E = 30 \text{ N}\cdot\text{m}$  was set for Condition 2, which is constant torque acting on the ship. A time-varying disturbance of  $N_E = 10\sin(0.2t) + 5\cos(0.5t)$  measured in  $\text{N}\cdot\text{m}$  was set for Condition 3. It represents the equivalent time-varying disturbance torque of the ship in  $z$  direction in marine environment, which is used to simulate disturbances caused by winds and waves to the ship's heading [20].

**Table 2 Simulation conditions**

| Condition   | Types of condition       | Types of simulation                      |
|-------------|--------------------------|--|
| Condition 1 | No disturbance           | Research on heading control              |
| Condition 2 | Constant disturbance     | Research on heading control              |
| Condition 3 | Time-varying disturbance | Research on heading and tracking control |

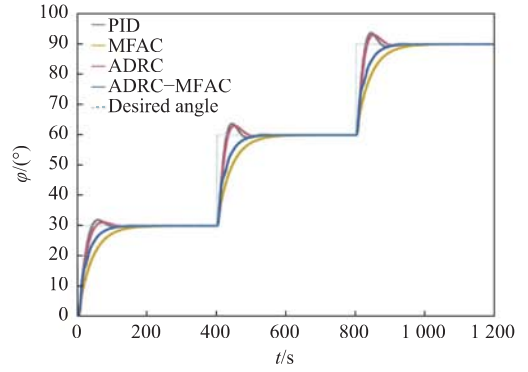
### 3.2 Simulation test of heading control

In this paper, simulation research of heading control was carried out under three working conditions: no disturbance, a constant disturbance, and a time-varying disturbance. The expected heading angle  $\varphi^*(k)$  was set as follows:

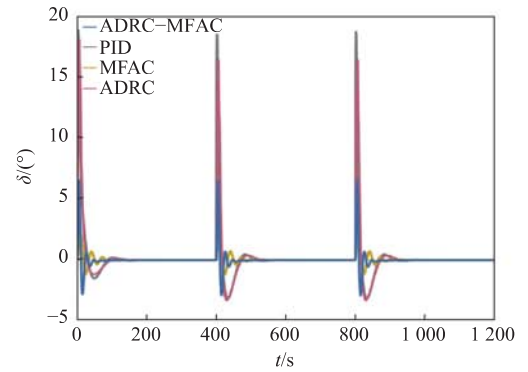
$$\varphi^*(k) = \begin{cases} 30^\circ, & 0 \leq t \leq 400 \\ 60^\circ, & 400 \leq t \leq 800 \\ 90^\circ, & 800 \leq t \leq 1200 \end{cases} \quad (19)$$

Fig. 7 illustrates simulated heading control under the four control algorithms in the case of no disturbance, and relevant system performance indexes are listed in Table 3. The results show that with no disturbance, the ship can adjust its heading in time and keep the expected course stably under all the four control algorithms. Specifically, the system has certain overshoot under the control of both PID and ADRC. Under the control of MFAC and ADRC-MFAC, it has no overshoot, with reduced steering

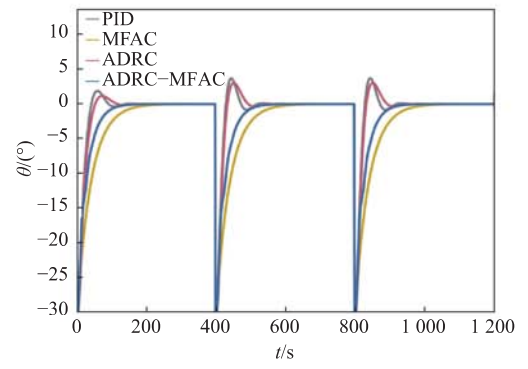
frequency and average rudder amplitude. The maximum rudder amplitude is  $4.23^\circ$  under MFAC and  $6.51^\circ$  under ADRC-MFAC control. As can be seen, after the introduction of MFAC, although the rise time is prolonged, rudder amplitude varies more smoothly, and ship navigation is more stable. Under condition 1, all the above four algorithms are basically in line with engineering requirements,



(a) Change in heading angle



(b) Rudder-angle control command



(c) Heading deviation

Fig. 7 Heading control effect without disturbance using different algorithms

**Table 3 Performance indexes of ship heading control system without disturbance for different algorithms**

| Algorithm | Rise time/s | Overshoot/( $^\circ$ ) | Steering frequency | Average rudder amplitude/( $^\circ$ ) |
|-----------|-------------|------------------------|--------------------|---------------------------------------|
| PID       | 25          | 3                      | 5.7                | 0.208                                 |
| MFAC      | 87          | 0                      | 4.35               | 0.054                                 |
| ADRC      | 27          | 2.5                    | 4.8                | 0.209                                 |
| ADRC-MFAC | 56          | 0                      | 4.2                | 0.043                                 |

despite slight difference in control effects.

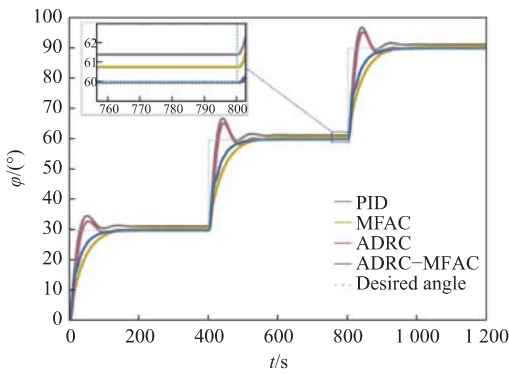
Fig. 8 compares simulation results of ship heading control in the case of constant disturbances, and relevant system performance indexes are listed in Table 4. The figure shows that heading control effect of each control algorithm is quite different after the addition of disturbances. For example, under PID, the heading angle deviates from the expected value by 1.396°, while the deviation is 0.74° under MFAC. Ship heading in both cases is affected by constant disturbances. Under ADRC, the system can identify and then compensated for the disturbances, thus improving the accuracy of heading control, with a steady-state heading deviation of less than 0.1°. However, there is a 4.56° overshoot and secondary oscillation. The system

**Table 4 Performance indexes of ship heading control system with constant disturbance for different algorithms**

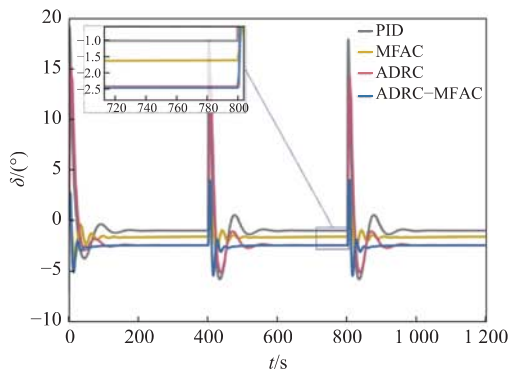
| Algorithm | Rise time/s | Overshoot/(°) | Steady-state deviation/(°) | Steady-state rudder amplitude/(°) |
|-----------|-------------|---------------|----------------------------|-----------------------------------|
| PID       | 21          | 6.165         | 1.396                      | -0.976                            |
| MFAC      | 80          | 0             | 0.765                      | -1.607                            |
| ADRC      | 24          | 4.560         | 0.024                      | -2.423                            |
| ADRC-MFAC | 55          | 0             | 0.007                      | -2.446                            |

has a maximum forward rudder angle of 14.23° and a maximum reverse rudder angle of -5.13°, with a large variation range. Under ADRC-MFAC, the system has a maximum forward rudder angle of 4.02° and a maximum reverse rudder angle of -5.37°, with a small variation range. Moreover, the heading angle does not overshoot. After entering a steady state, the system keeps rudder amplitude at about -2.446° to overcome the influence of constant disturbances, with basically no heading deviation.

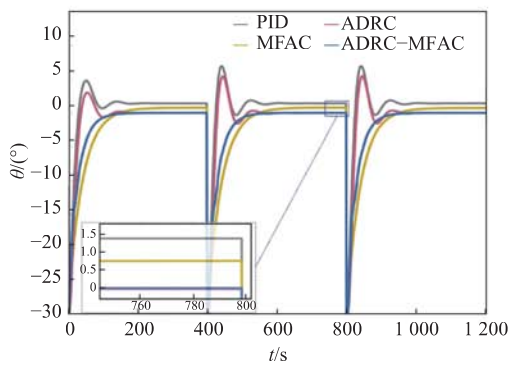
Fig. 9 compares simulation results of ship heading control in the case of time-varying disturbances, and relevant system performance indexes are reported in Table 5. The results show that after the addition of time-varying disturbances, the ship's heading fluctuates around the target, with greatly reduced stability. Among the four algorithms, ADRC-MFAC yields the smallest steady-state deviation of heading angles, the lowest average



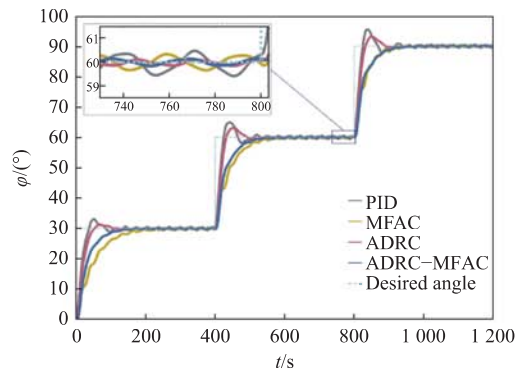
(a) Variation curve of heading angle



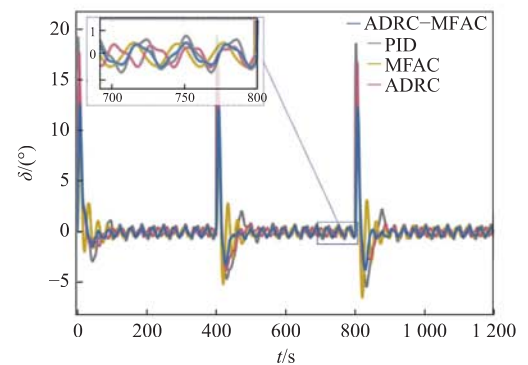
(b) Rudder-angle control command



(c) Heading deviation



(a) Change in heading angle



(b) Rudder-angle control command

Fig. 8 Heading control effect with constant disturbance using different algorithms

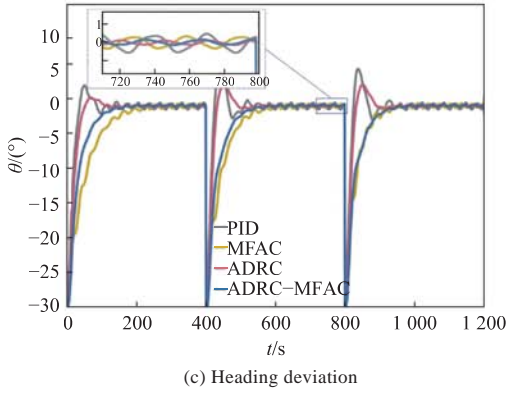


Fig. 9 Heading control effect under time-varying disturbance using different algorithms

**Table 5 Performance indexes of ship heading control system under time-varying disturbance for different algorithms**

| Algorithm | Rise time/s | Overshoot/(°) | Average deviation/(°) | Average rudder amplitude/(°) |
|-----------|-------------|---------------|-----------------------|------------------------------|
| PID       | 22          | 4.864         | 0.361                 | 1.090                        |
| MFAC      | 92          | 0             | 0.376                 | 0.714                        |
| ADRC      | 22          | 3.061         | 0.196                 | 0.859                        |
| ADRC-MFAC | 67          | 0             | 0.184                 | 0.623                        |

rudder amplitude, no overshoot, and thus the most stable control effect.

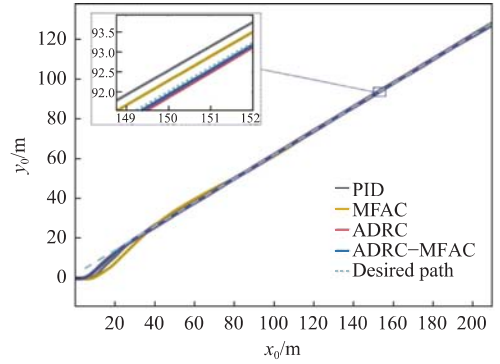
In a nutshell, the ADRC-MFAC algorithm can effectively adjust rudder-angle amplitude and steering frequency to ensure steady variation of heading. The results verify the effectiveness of the proposed algorithm for ship heading control.

### 3.3 Simulation test of tracking control

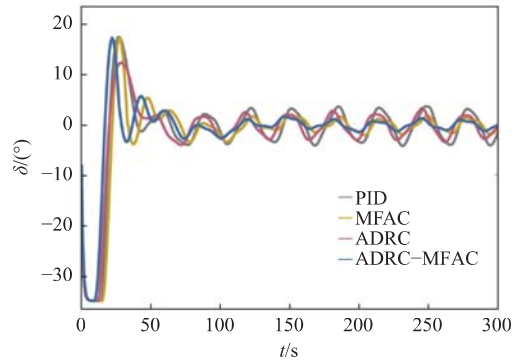
Based on the simulation research of heading control, time-varying disturbances were introduced for simulation research of tracking control. Specifically, four algorithms were used for simulation tests of straight- and curve-track control, respectively.

Fig. 10 illustrates the control effect of the ship following a straight track under external time-varying disturbances. Table 6 reports relevant system performance indexes. At the initial stage, the ship turns sharply to sail to the preset track in all cases, with little time difference in sailing along the preset track to reach the destination after approaching the track. Rudder-angle control commands fluctuate obviously under the influence of time-varying disturbances. However, after the introduction of MFAC, rudder-angle variation of the system is controlled, with average rudder amplitude being reduced. Tracking accuracy of the system is also affected by time-varying disturbances. Compara-

tively, as ADRC and ADRC-MFAC controllers can observe and estimate internal and external disturbances through the ESO, the system compensates for the disturbances, resulting in higher tracking accuracy and better control performance.



(a) Navigation track of ship



(b) Rudder-angle control command

Fig.10 Straight-path following control effect under time-varying disturbance using different algorithms

**Table 6 Performance indexes of ship straight-path following control system under time-varying disturbance for different algorithms**

| Algorithm | Arrival time/s | Average rudder amplitude/(°) | Average tracking deviation/m | Maximum tracking deviation/m |
|-----------|----------------|------------------------------|------------------------------|------------------------------|
| PID       | 281            | 4.593                        | 0.149                        | 0.672                        |
| MFAC      | 273            | 3.745                        | 0.164                        | 1.185                        |
| ADRC      | 276            | 3.939                        | 0.087                        | 0.383                        |
| ADRC-MFAC | 272            | 2.890                        | 0.056                        | 0.291                        |

Fig. 11 illustrates the control effect of curve-track following. Table 7 reports relevant system performance indexes. As can be seen, the ship under MFAC is obviously affected by disturbances, with a large tracking deviation. The system under conventional PID control also needs to correct rudder angle frequently to keep itself from deviating from the expected track, with excessively large rudder amplitude. ADRC and ADRC-MFAC can obviously reduce the impact of external disturbances on the system. With these algorithms, the ship sails more smoothly along the preset track, with short deviation

distance and high control accuracy. Specifically, ADRC-MFAC yields smoother rudder-angle variation and better control effect.

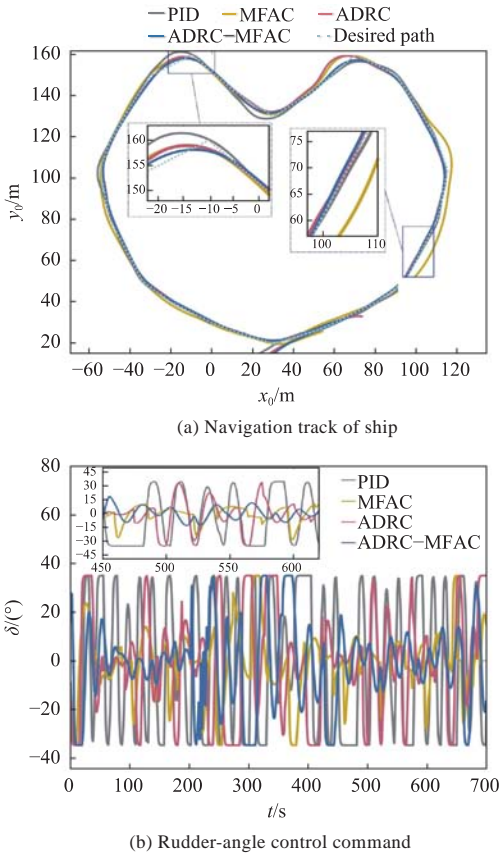


Fig.11 Curved-path following control effect under time-varying disturbance using different algorithms

**Table 7 Performance indexes of ship curved-path following control system under time-varying disturbance for different algorithms**

| Algorithm | Arrival time/s | Average rudder amplitude/( $^{\circ}$ ) | Average tracking deviation/m | Maximum tracking deviation/m |
|-----------|----------------|---|------------------------------|------------------------------|
| PID       | 662            | 15.028                                  | 0.631                        | 5.239                        |
| MFAC      | 689            | 10.756                                  | 1.869                        | 6.601                        |
| ADRC      | 639            | 12.601                                  | 0.297                        | 5.462                        |
| ADRC-MFAC | 654            | 9.520                                   | 0.281                        | 3.317                        |

In conclusion, ADRC-MFAC can achieve good ship heading and tracking control. By disturbance compensation, it reduces impact of complex environmental disturbances on systems, with faster response and more stable dynamic performance. Thus, it is more in line with actual needs.

## 4 Conclusions

Considering the impact of complex environment disturbances on ship sailing, in view of tracking control, this paper proposed an ADRC-MFAC-based algorithm for ship motion control. In addition, simulation analysis was carried out by

taking the KVLCC2 under-actuated tanker model ship as an example. The results show that the ADRC-MFAC algorithm can realize stable ship heading and tracking control under complex environmental disturbances. The algorithm proposed in this paper is independent of an accurate model and applicable to ships with uncertain parameters or unknown external inputs, thus effectively improving capabilities of ships against complex environmental disturbances. Compared with conventional control algorithms such as PID, MFAC, and ADRC, this algorithm has more accurate control and faster response. We will introduce reinforcement learning in later research to study parameter self-tuning of ADRC-MFAC, so as to enhance adaptability of this algorithm to different controlled ships.

## References

- [1] YAN X P. Research status and development trend of intelligent ship[J]. *Communication & Shipping*, 2016(1): 23–26 (in Chinese).
- [2] ZHANG X F, YUAN P, TAN J Z, et al. Heading control method of unmanned sailing boats based on fuzzy PID[J]. *Chinese Journal of Ship Research*, 2019, 14(6): 15–21 (in both Chinese and English).
- [3] WITKOWSKA A, ŚMIERZCHALSKI R. Designing a ship course controller by applying the adaptive backstepping method[J]. *International Journal of Applied Mathematics and Computer Science*, 2012, 22(4): 985–997.
- [4] SUN J. Research on the sliding mode control for under-actuated surface vessels via parameter estimation[J]. *Nonlinear dynamics*, 2018, 91: 1163–1175.
- [5] JIMOH I A, KUUKDEMIRAL I B, BEVAN G. Fin control for ship roll motion stabilisation based on observer enhanced MPC with disturbance rate compensation[J]. *Ocean Engineering*, 2021, 224(4): 108706.
- [6] HUANG J W, GAO J W. How could data integrate with control? a review on data-based control strategy [J]. *International Journal of Dynamics and Control*, 2020, 8(4): 1189–1199.
- [7] FORMENTINN S, VAN H, KARIMI A. A comparison of model-based and data-driven controller tuning[J]. *International Journal of Adaptive Control and Signal Processing*, 2014, 28(10): 882–897.
- [8] HAN J Q. Active disturbance rejection controller technology[J]. *Frontier Science*, 2007(1): 24–31(in Chinese).
- [9] MIAO X, ZHAO H, GAO B, et al. Motion analysis and control of the pipeline robot passing through girth weld and inclination in natural gas pipeline[J]. *Journal of Natural Gas Science and Engineering*, 2022: 104662.
- [10] LAGHRIDAT H, ESSADKI A, NASSER T. Co-ordinated control by ADRC strategy for a wind farm based on SCIG considering low voltage ride-through capability

- ity[J]. Protection and Control of Modern Power Systems, 2022, 7(1): 1–18.
- [11] XIONG H J, LIU J Y, CHEN Y P. Simulation research on ship dynamic positioning control based ADRC under strong interference environment[J]. Journal of Wuhan University of Technology, 2015(3): 52–57 (in Chinese).
- [12] HUANG H, FAN Y. Path following for unmanned surface vessels based on adaptive LOS guidance and ADRC[C]//Processings of the 24th International Conference on Neural Information. Guangzhou, China: Springer International Publishing, 2017: 192–200.
- [13] LIAO Y, JIANG Q, DU T, et al. Redefined output model-free adaptive control method and unmanned surface vehicle heading control[J]. IEEE Journal of Oceanic Engineering, 2019, 45(3): 714–723.
- [14] LIU S, HOU Z, Li Z. Data-driven model-free adaptive control based on a novel double successive projection algorithm[C]//Proceedings of the 14th IEEE International Conference on Control, Automation, Robotics and Vision (ICARCV). Phuket, Thailand: IEEE, 2016: 1–6.
- [15] YI Z, LIANG T, CHAO L, et al. Wide-area power system stabiliser based on model-free adaptive control[J]. IET Control Theory and Applications, 2015, 9(13): 1996–2007.
- [16] PANG Z, LIU G P, ZHOU D, et al. Data-based predictive control for networked nonlinear systems with network-induced delay and packet dropout[J]. IEEE Transactions on Industrial Electronics, 2016, 63(2): 1249–1257.
- [17] ZHANG G, ZHANG X. A novel DVS guidance principle and robust adaptive path-following control for underactuated ships using low frequency gain-learning [J]. Isa Transactions, 2015, 56: 75–85.
- [18] CHEN Z, XUE Q, LUO K, et al. Intelligent automatic control of ship berthing with improved LOS guidance [J]. Navigation of China, 2021, 44(2): 126–133 (in Chinese).
- [19] LIU J, QUADVLIEG F, HEKKENBERG R. Impacts of the rudder profile on manoeuvring performance of ships[J]. Ocean Engineering, 2016, 124: 226–240.
- [20] ZHAO Z P, ZHANG Q. Adaptive self-regulation PID tracking control for the ship course[J]. Chinese Journal of Ship Research, 2019, 14(3): 145–151 (in both Chinese and English).

## 船舶自抗扰无模型自适应航迹控制

李诗杰<sup>1,2,5</sup>, 徐诚祺<sup>5</sup>, 刘佳仑<sup>\*1,2,3,4</sup>, 徐子茜<sup>5</sup>, 孟凡彬<sup>2,6</sup>

1 武汉理工大学 水路交通控制全国重点实验室, 湖北 武汉 430063

2 中国船舶航海保障技术实验室, 天津 300131

3 武汉理工大学 智能交通系统研究中心, 湖北 武汉 430063

4 国家水运安全工程技术研究中心, 湖北 武汉 430063

5 武汉理工大学 交通与物流工程学院, 湖北 武汉 430063

6 天津航海仪器研究所, 天津 300131

**摘要:** [目的] 旨在研究船舶在真实海况下航行面临复杂环境干扰的影响, 控制船舶克服干扰, 实现航迹跟随、智能航行。 [方法] 首先, 将无模型自适应控制(MFAC)算法引入自抗扰控制器(ADRC)中, 设计改进自抗扰无模型自适应控制(ADRC-MFAC)算法, 通过ADRC跟踪系统的实时状态、识别系统所受未知扰动, 根据MFAC建立输入数据(舵角)与输出数据(航向角、角速度)之间的非线性关系, 实现稳定的航向控制。然后, 结合自适应视线(LOS)制导策略, 通过动态航向控制实现对航迹的精准控制。 [结果] 仿真结果表明, 所设计的控制器能够控制船舶快速航行至预设轨迹并沿轨迹行进, 在复杂环境扰动下仍能够实现理想的航迹控制。 [结论] 研究成果不依赖船舶具体模型, 可为船舶航迹控制提供参考。

**关键词:** 航迹控制; 自抗扰控制算法; 无模型自适应控制算法; 数据驱动控制